CONF-960608--7

ISOTHERMAL AND CYCLIC OXIDATION OF AN AIR PLASMA-SPRAYED THERMAL BARRIER COATING SYSTEM

J. Allen Haynes, Mattison K. Ferber, Wallace D. Porter
High Temperature Materials Laboratory
Oak Ridge National Laboratory
Oak Ridge TN 37831-6069

E. Douglas Rigney
Department of Materials and Mechanical Engineering
University of Alabama at Birmingham
Birmingham, AL 35294

ABSTRACT

Thermogravimetric methods for evaluating bond coat oxidation in plasma-sprayed thermal barrier coating (TBC) systems were assessed by high-temperature testing of TBC systems with air plasma-sprayed (APS) Ni-22Cr-10Al-1Y bond coatings and yttria-stabilized zirconia top coatings. High-mass thermogravimetric analysis (at 1150°C) was used to measure bond coat oxidation kinetics. Furnace cycling was used to evaluate APS TBC durability. This paper describes the experimental methods and relative oxidation kinetics of the various specimen types. Characterization of the APS TBCs and their reaction products is discussed.

INTRODUCTION

Ceramic thermal barrier coatings (TBCs) are commonly applied to air-cooled gas turbine engine components in order to extend service lifetimes by reducing metal temperatures and decreasing the severity of hot spots. A typical TBC system consists of a thermally insulating ceramic top coating (with good strain tolerance) deposited over an oxidation-resistant metallic bond coating. The most common ceramic thermal barrier material is 6 - 8 weight % yttria-stabilized zirconia (YSZ), applied by air plasma-spraying (APS).

The thermal protection offered by the ceramic top coating also has the potential to provide improved efficiencies to gas turbine engines by permitting significant increases in turbine inlet temperatures or decreases in cooling air. However, current TBC systems eventually fail by spallation of the YSZ layer. Integration of the TBC thermal benefit into advanced turbine designs would involve substantial risk, since loss of the ceramic protection at significantly elevated operating temperatures would result in rapid degradation of the underlying metallic component. An improved understanding of TBC degradation and failure mechanisms is necessary for development of more reliable coating systems (Miller, 1987; Parks et. al, 1995).

It is generally agreed that TBC failure is primarily influenced by, (1) thermal expansion mismatch stresses between the metal and ceramic layers, and (2) the effects of various thermally activated processes such as sintering, creep, diffusion, and bond coat oxidation (Miller, 1984; Hillery et. al., 1988; DeMasi et. al. 1989; Wortman et. al., 1989; Meier et. al., 1991). It has been reported that high-temperature oxidation of the bond coating plays a major role in TBC degradation (Miller, 1984; Wu et. al., 1989; Meier et. al., 1991). However, the mechanisms by which oxidation affects TBC life are still not well understood (Miller, 1989; Mevrel, 1989). It is likely that as inlet temperatures and operating cycle lengths (in land-based turbines) continue to increase, the role of thermally activated degradation processes such as bond coat oxidation will also increase.

Bond coatings generally consist of an MCrAlY (M = Ni and/or Co) alloy, and are applied by either APS or low pressure plasma spraying (LPPS). During high temperature operation the bond coat

DISCLAIMER

alloy reacts with oxygen (which is rapidly transported through the YSZ layer) to form a dense oxide scale (which also protects the superalloy) at the bond coat/YSZ interface. Continued growth of this scale contributes to the eventual failure of the YSZ top coating. An increased basic understanding of the mechanisms and kinetics of bond coat oxidation should be a valuable resource for improving the reliability of long term TBC life prediction models, and may provide insight into manufacturing and materials advancements.

The overall aim of this work is to develop an improved understanding of bond coat oxidation and its role in TBC degradation and failure. Objectives of this preliminary study were; (1) develop thermogravimetric methods for careful evaluation of bond coat oxidation, and (2) evaluate these methods by investigating the oxidation of a commercial APS TBC system under accelerated conditions. Future work will evaluate oxidation of electron beam-physical vapor deposition (EB-PVD) TBC systems.

EXPERIMENTAL PROCEDURES

Materials

Superalloy discs (2.54 cm diameter by 0.3175 cm thickness) with chamfered edges were machined from nickel-based superalloy, and used for all specimen substrates. Substrates were coated with APS TBCs by a commercial source, using proprietary plasma-spray parameters. All bond coatings were identically deposited to a nominal thickness of 125 μm using NiCrAlY powders (-140 +270 mesh). Table 1 lists the compositions of the bond coat alloy and superalloy. Top coatings were applied to a nominal thickness of either 250 μm or 500 μm, and consisted of ZrO_2-8 wt% Y_2O_3.

Table 1. Superalloy and Bond Coat Chemistry (wt %)

	Ni	Cr	Al	Y	Co	Mo	Ti	Fe
Waspaloy *	Bal	19.3	1.4	*	12.5	3.9	2.9	1.1
NiCrAlY	Bal	22.0	10.0	1.0	*	*	*	*

* The superalloy also contained less than 0.10 wt % of: Zr, Si, Mn, Cu, Cb, Ta, and P. S was reported as 0.003 wt%.

Isothermal Oxidation Experiments

Four types of specimens (Table 2) were prepared for thermogravimetric analysis (TGA). Surfaces of the Type A specimens (bare superalloy) were in the as-machined condition. The Type B, C and D TGA specimens were coated on both faces, with edges not coated.

Table 2. TGA Specimen Descriptions

Type	Bond Coating	Top Coating	Comment
A	none	none	bare substrate
B	125 μm NiCrAlY	none	both faces coated
C	125 μm NiCrAlY	250 μm YSZ	both faces coated
D	125 μm NiCrAlY	500 μm YSZ	both faces coated

Oxidation weight gains were measured by continuous thermogravimetry using an ATI/Cahn TG-171 high-mass TGA system with a vertical tube furnace. Tests were conducted at 1150°C (± 3°C) in dry air flowing at 100 cm^3min^{-1}. Specimens were suspended from a sapphire hanger in a Pt - Rh wire basket. They were heated in the reaction gas at a rate of 50°C/min, isothermally held for up to 100 hours, and cooled to room temperature at an average rate of 8.0°C/min. Specimen masses were recorded continuously by a microprocessor. Isothermal testing of substrates coated on one face was conducted for 1 to 200 hours in a box furnace at 1150°C.

Thermal Cycle Testing

Durability of the APS TBCs was evaluated by thermal cycle testing in a programmable, microprocessor-controlled furnace. Specimens were coated on one face with the APS bond coating, and either a 250 μm or a 500 μm APS top coat. Thermal cycles consisted of a 15 minute heat-up to 1150°C (± 3°C), a 60 minute isothermal hold at 1150°C in still air, and forced air cooling for 30 minutes to 90°C. Specimens were examined at 12 cycle intervals. Selected specimens were isothermally pre-oxidized at 1150°C for 100 hours.

Characterization

Oxide phases were identified by x-ray diffraction (XRD) using Cu k_α radiation at 40 mA and 45 kV. Coatings and reaction products were evaluated via field emission gun-scanning electron microscopy (FEG-SEM) with energy dispersive spectroscopy (EDS) at 15 kV. Compositional profiles and x-ray maps were obtained by electron microprobe analysis (EPMA) at 15 kV.

RESULTS AND DISCUSSION

Isothermal oxidation weight gains of the four types of TGA specimens are plotted as parabolic curves (specific weight gain *vs.* square root time) in Figs. 1(a) - (d). The scatter in oxidation weight gains was expected, due to the non-homogeneous structure of the APS bond coatings. This structure is shown in Figs. 2(a) and (b), which are cross-sectional SEM micrographs of the bond coat region

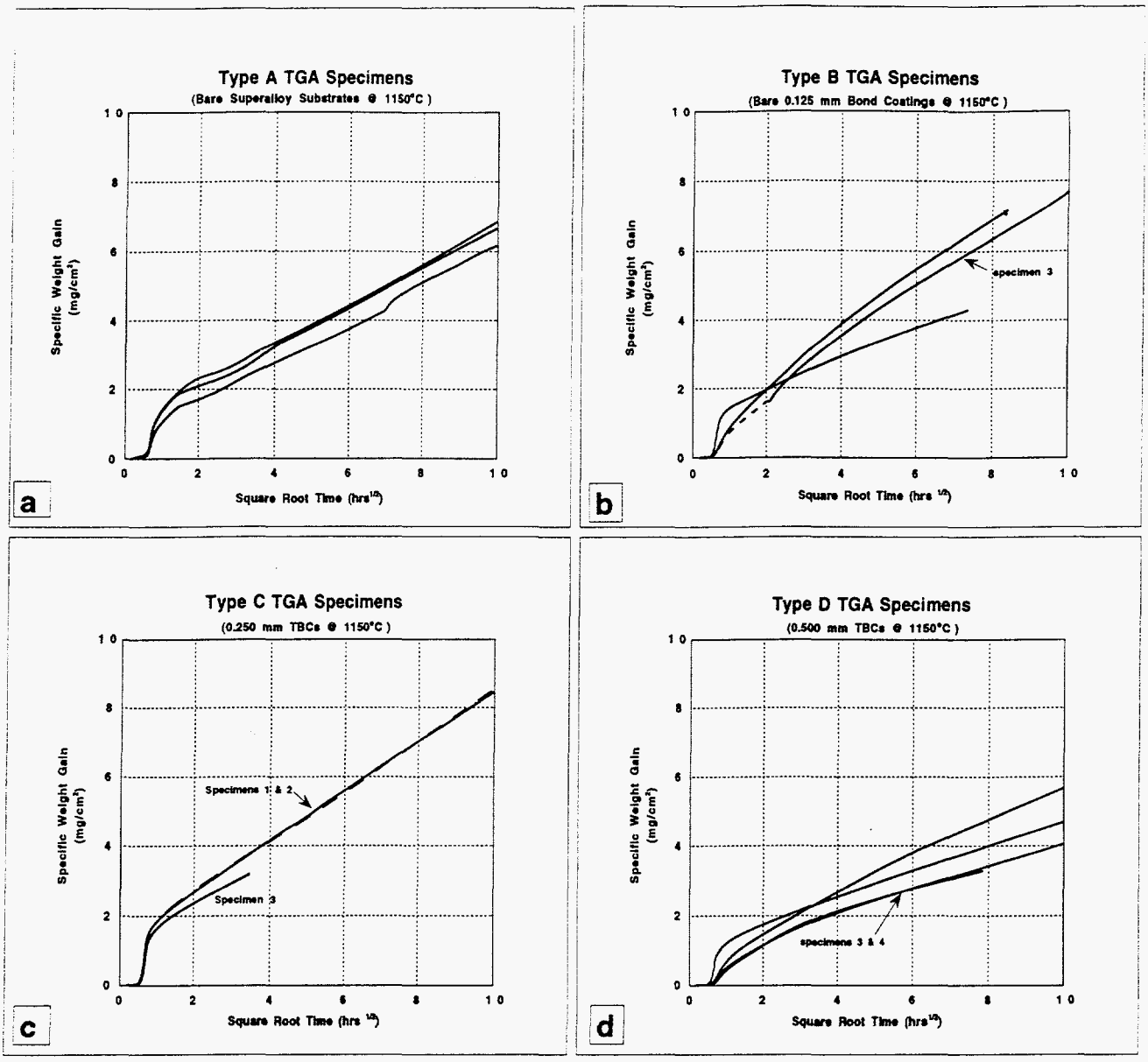

Fig. 1. Parabolic plots of isothermal oxidation weight gains of the four types of TGA specimens (a) bare substrates, (b) bare NiCrAlY, (c) 250 μm TBC, and (d) 500 μm TBC. The oxidation rates for the Type A specimens were actually much higher than the other specimens, since the surface area of these relatively smooth, dense substrates was much lower than that of the specimens with the rough, porous APS NiCrAlY coatings.

of Type C specimens. As can be seen in Fig. 2(a), the as-deposited bond coatings displayed significant internal porosity (both spherical and interlamellar), oxide stringers (from reactions during plasma spraying in air), and a convoluted bond coat/YSZ interface.

The rough bond coat surface, which is necessary for mechanical "keying" of the plasma-sprayed ceramic, results in significantly increased metallic surface area over which oxidation occurs. Figure 2(b) shows the significant scale growth which occurred at the

Table 3. TGA Test Conditions and Effective Parabolic Oxidation Rate Constants (at 1150°C)

Specimen	Coating	Time (hrs)	k_p' ($mg^2cm^{-4}h^{-1}$)
A-1	none	100	0.3313
A-2	none	100	0.3403
A-3	none	100	0.3365
B-2	NiCrAlY	54	0.5289
B-3	NiCrAlY	4 + 96*	0.4635
B-4	NiCrAlY	72	0.6591
C-1	250 μm TBC	100	0.5172
C-2	250 μm TBC	100	0.5289
C-3	250 μm TBC	48	0.3667
D-1	500 μm TBC	100	0.2707
D-2	500 μm TBC	100	0.1350
D-3	500 μm TBC	61	0.1118
D-4	500 μm TBC	100	0.1224

† Some runs aborted short of 100 hrs by power outages and software errors.
* B-3 was aborted by power outage, and then tested an additional 96 hours.

interface, along internal porosity and at splat boundaries.

After correction for buoyancy and Pt evaporation, oxidation rate constants (k_p) were estimated from the steady-state portions of the parabolic plots in Figs. 2(a) - (d). The oxidation rate constant is generally defined by the equation $(\Delta m/A)^2 = k_p t$, where $\Delta m/A$ denotes weight gain per unit surface area (specific weight gain) and t is the oxidation period. The actual surface area over which NiCrAlY oxidation occurred was unknown, due to the bond coat surface roughness and scale growth along internal porosity. Since all bond coatings were sprayed with the same parameters, the assumption was made that all bond coat surface areas were approximately equal, and the surface area of a flat substrate disc was used as an estimate of A. This resulted in an effective oxidation rate constant k_p' (Table 3) which was higher than actual for the coated specimens. Additional error was introduced by oxidation and spallation along the bare substrate edges (which comprised less than 10% of the total substrate surface area). These k_p' values were for use on a comparative basis in this study, and are not to be interpreted as absolute NiCrAlY oxidation rates.

Oxidation of Type A Specimens (Bare Superalloy)

Oxidation curves for the bare substrates (Fig. 1a) displayed irregularities which may be indicative of scale cracking, spallation, volatilization, or the growth of differing oxide species. Upon cooling to room temperature significant spallation weight losses were measured. X-ray diffraction indicated the major surface oxide was Cr_2O_3, which is volatile above 1000°C. Spall products consisted of TiO_2, Cr_2O_3 and NiO (by XRD).

Oxidation of Type B Specimens (Bare NiCrAlY)

Oxidation weight gains of the NiCrAlY-coated specimens are plotted in Fig. 1(b). The steady-state portions of the curves were near parabolic in nature, indicating predominately diffusion-controlled scale formation. Rapid weight gains typically occur during the initial stage of high-temperature oxidation due to the formation of non-protective oxides with rapid growth kinetics. In alloys that form a protective scale, a continuous layer of a dense,

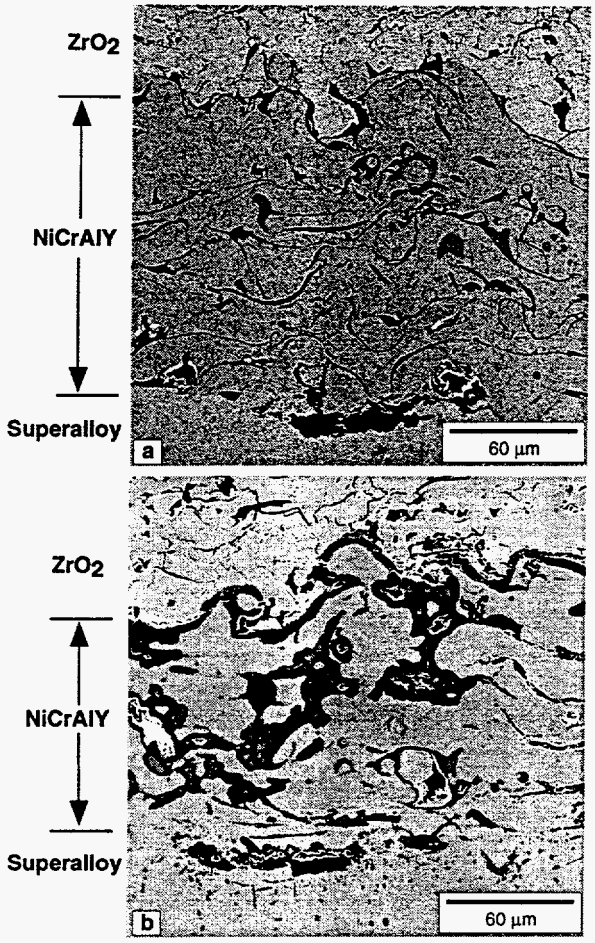

Fig. 2. Secondary electron images of the bond coatings from Type-C specimens. (a) As-deposited, note the oxide stringers, porosity, and rough interface. (b) 100 hrs at 1150°C, note the significant interfacial and internal oxidation.

protective oxide (such as Al_2O_3) with slower growth kinetics eventually forms beneath the transient oxides, and the oxide growth kinetics then decrease to steady-state parabolic rates (Prescott and Graham, 1992).

No oxides were detected by XRD of the as-sprayed bond coats. After 1, 100 and 200 hours isothermal oxidation, XRD indicated α-Al_2O_3 (JCPDS 42-1468) as the major oxide phase, with lesser amounts of $Al_5Y_3O_{12}$ (JCPDS 33-40) and $NiAl_2O_4$ (JCPDS 10-339). Spall products consisted of Cr_2O_3, NiO and TiO_2 (from the substrate edges). The majority of the bond coat surface scale remained intact.

Oxidation of Type C Specimens (250 μm TBCs)

As shown in Fig. 1(c) specimens with 250 μm top coatings also displayed near parabolic steady-state weight gains. There were moderate weight losses during cooling, with spall products again consisting of Cr_2O_3, NiO and TiO_2 (from the substrate edges). No spallation of the YSZ occurred.

Figure 3 is a cross section of a Type C specimen after 100 hours oxidation, and shows the variable amounts of internal oxidation which occurred in the bond coat. The top coating displays the porous, microcracked structure typical of plasma-sprayed YSZ. Figure 4(a) is a higher magnification image of the interfacial scale. A microcrack (arrow) extends through the scale at the bond coat peak, which is a region of high tensile stress.

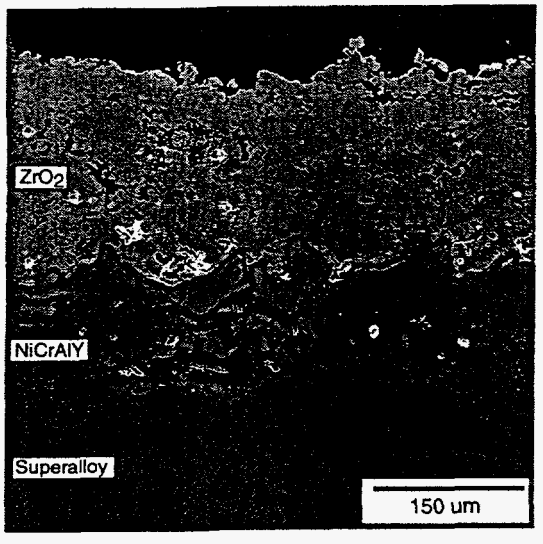

Fig. 3. Type C specimen cross section after 100 hours oxidation (1150°C). Note the porous ceramic top coating (which also remained intact after 200 hours testing). The bond coat displayed widely varying amounts of internal oxidation from location to location.

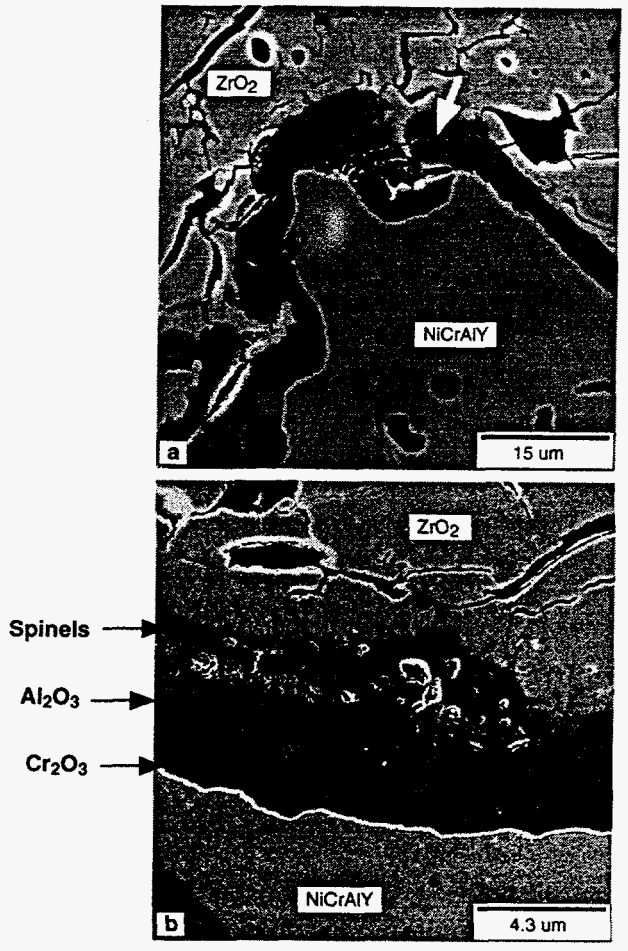

Fig. 4. Secondary electron images of a Type-C bond coat/top coat interface after 100 hrs at 1150°C. (a) The arrow shows a crack which propagated through the scale at the bond coat peak, (b) Magnified view showing the three discrete layers of interfacial reaction products.

X-ray maps of the elements Al and Y (Fig. 5) were obtained by EPMA of specimen cross sections in the bond coat region of an as-deposited specimen and a specimen oxidized for 100 hours. These compositional maps indicated, (1) the internal oxides of the as-deposited bond coatings contained Al and/or Y, (2) the Al content in the oxidized bond coat was depleted due to scale formation and

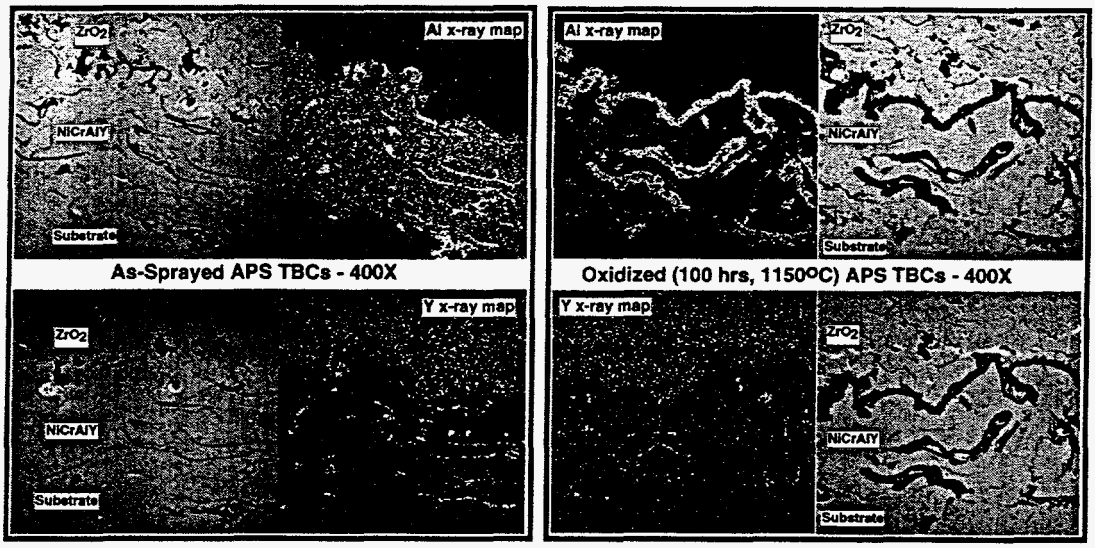

Fig. 5. Microprobe X-ray compositional maps of the elements Al and Y. (a) As-deposited Type C TBC with Al and Y-rich bond coat oxide stringers. (b) Same type specimen after 100 hrs oxidation (1150°C). Note the Al depletion in the bond coat matrix, and Y concentrated in the internal oxides.

interdiffusion with the substrate, (3) Al was segregated as Al_2O_3 at the bond coat/YSZ interface after oxidation, and (4) after oxidation the bulk of the Y remained as internal oxides.

Figure 6(a) is a microprobe line profile which shows the compositional variation across the bond coat of an as-deposited specimen. The O, Al, and Y concentrations in the bond coat are internal oxide stringers which formed due to reaction during the high-temperature APS process. The normalized weight percent of Al measured in the bond coat was approximately 9.5 wt%. Figure 6(b) is a microprobe line profile across a bond coat after 100 hours oxidation. Aluminum concentrated at the interface, and in the internal oxides (with Y). The Al concentration in the bond coat was reduced to approximately 1.3 wt%, and significant amounts of Co (2.8 wt%) and Ti (0.30 wt%) diffused into the bond coat.

Field-emission SEM of the interfacial reaction products after 100 hours oxidation revealed a continuous scale consisting of one to three layers. The total scale thickness varied from 2.6 to 12.0 μm, with an average of approximately 4.9 μm. All three layers are shown in Fig. 4(b). The predominant reaction product was the darker contrast oxide in the central region of the scale. Field-emission EDS identified this layer as Al_2O_3, with traces of Zr, Y and Cr. Alumina was present at all points along the interface as a dense continuous layer, with intermittent through cracking. Thickness of the Al_2O_3 varied from 2.6 to 7.0 μm.

The lighter contrast oxide layer adjacent to the YSZ in Fig. 4(b) was intermittently present over the majority of the interface, and contained Al, O, Cr and Ni. After 100 hours its thickness varied from 0.0 - 5.0 μm. From XRD of the oxidized bare bond coatings, as well as previous work (Alperine and Lelait, 1994), it was concluded that this oxide layer consisted primarily of $Ni(Al,Cr)_2O_4$ spinels. A very thin spinel layer was present in a specimen oxidized for 1 hour. A much thicker spinel layer (0.0 to 10 μm) was present in a specimen which remained intact after 200 hours oxidation, indicating continued growth of the spinel through the Al_2O_3. The presence of the spinels at the interface did not appear to degrade the adhesion of the YSZ under isothermal conditions.

A third oxide layer was detected at a few locations along the interface. As shown in Fig. 5(b) this thin lighter-contrast layer was adjacent to the NiCrAlY, and varied in thickness from 0 - 0.5 μm. Evaluation by EDS indicated Cr_2O_3, which is not thermodynamically preferred at 1150°C. Alperine and Lelait (1994) reported an interfacial scale bordered on the NiCrAlY side by a fine layer of pure chromia after 100 hours oxidation of a similar system at 1200°C. Due to the convoluted interfacial geometry, the Cr_2O_3 may have formed in regions of localized Al depletion (such as at bond coat peaks where three dimensional outward diffusion would cause more rapid solute depletion) with insufficient Al flux to maintain Al_2O_3.

Two predominant types of internal oxides were noted (Fig.

2b) after 100 hours. The darker contrast oxides were Al_2O_3, formed by reaction with oxygen along porosity and splat boundaries. The lighter contrast internal oxide pockets contained Y and Al (and trace amounts of Ti), and were likely remnants of the oxide stringers in Fig. 2(a). Many of these Y-rich oxide pockets were enveloped by Al_2O_3, as pointed out by the arrow in the composition profile of Fig. 6(b). Since XRD of the oxidized bare bond coatings detected $Al_5Y_3O_{12}$ (YAG), and the majority of Y was in the internal oxides, it was concluded that the light-contrast internal oxides were predominately YAG. The influences of YAG formation on TBC durability are not clear.

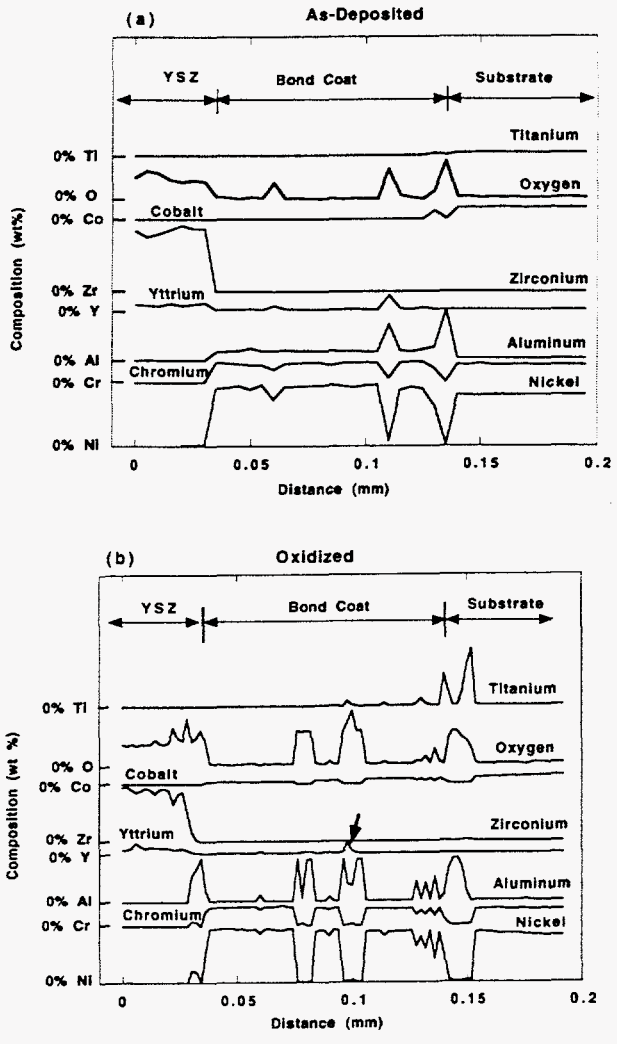

Fig. 6. Microprobe compositional line traces. (a) As-sprayed, note the internal Al-Y oxides, (b) Oxidized 100 hrs. Other areas of the bond coat contained larger amounts of internal Y-oxides.

Oxidation of Type D Specimens (500 μm TBCs)

Oxidation weight gains for the Type D TBC specimens (Fig. 1d) displayed a mean k_p' (Table 3) that was statistically lower (by the Student t-test) than the means of the other two types of coated specimens (which were not statistically different). The scales of the Type D specimens were similar to those discussed for the Type C specimens, with an average interfacial thickness of 5.2 μm.

A TGA study conducted by Brindley and Miller (1990) measured average k_p values of approximately 0.014 $mg^2cm^4h^{-1}$ at 1083°C in pure O_2 for monolithic LPPS Ni-18Cr-12Al-0.3Y specimens coated with APS YSZ. The rates measured for TBC-coated specimens in this study are 10 to 35 times higher (without correction of the kp' errors discussed previously). However, after consideration of the 67°C temperature increase, as well as the differences in the LPPS NiCrAlY density and chemistry, the NiCrAlY oxidation kinetics in this study are on the order of those reported previously.

Some authors have suggested the YSZ may affect oxidation kinetics by lowering the partial pressure of oxygen at the interface (Bennett, 1986; Wu et. al. 1989), or by modification of the scale growth mechanisms by solid state reactions with the additional reactive elements (Y and Zr) provided by the YSZ (Lelait et. al., 1992). Due to uncertainties introduced by surface area assumptions, internal oxidation and edge spallation, no specific conclusion could be made regarding the effects of the YSZ on the NiCrAlY oxidation rates in this study.

Thermal Cycling Experiments

Results of thermal cycle testing are shown in Table 4. Failure was defined as visible delamination or spallation of the YSZ. The 250 μm TBCs failed by buckling and partial delamination of a small section of the ceramic adjacent to the substrate edge (where severe substrate degradation occurred). The 500 μm TBCs failed by delamination of the entire YSZ layer as one monolithic piece. The average lifetime was equal for both TBC types (tested as-received). However, the thinner TBCs failed over less than 10% of the surface, whereas the thicker specimens failed over the entire surface. Oxidizing pre-treatments decreased the cyclic life of both types of coatings, with a greater decrease occurring for the thicker TBC. Failure modes were not altered by the pre-treatment. These APS TBCs displayed lifetimes on the order of those reported for TBCs with LPPS bond coatings tested at 1135°C (Wortman et. al., 1989).

Delamination of the 500 μm YSZ top coatings occurred in the YSZ, but near the interface. X-ray diffraction detected only ZrO_2 on the spalled YSZ fracture surfaces; and ZrO_2 with slight amounts of

Table 4. Results of Thermal Cycle Testing

Sample	YSZ Thickness	Pre-Treat	Cycles to Failure	Time at Temp.	Failure Mode†
1	250 μm	none	168	168 hrs	A
2	250 μm	none	132	132 hrs	A
3	250 μm	100 hrs	84	184 hrs	A
4	500 μm	none	144	144 hrs	B
5	500 μm	none	156	156 hrs	B
6	500 μm	100 hrs	60	160 hrs	B

†A=buckling and delamination of YSZ at one point on edge of specimen
†B = complete delamination of the YSZ as one monolithic piece

$NiAl_2O_4$ and Al_2O_3 on the substrate side of the failure surfaces. Evaluation of the spalled YSZ failure surfaces by SEM/EDS indicated small pockets of Al-, Cr- and Ti- containing oxides (with small amounts of Ni) of varying morphologies. The specimens which received the 100 hour isothermal pre-treatment displayed significantly greater amounts of Ti-containing oxides, likely due to increased diffusion of this active element from the substrate during the pre-treatment. Evaluation of the substrate side of the failure surfaces by SEM/EDS revealed scattered pockets of oxidation products protruding through the fractured YSZ. The surface oxides contained Al, Ti, Cr and O, with lesser amounts of Ni. Some areas of intact Al_2O_3 were exposed. In the pre-oxidized specimen Ti-containing oxides were common, which may have been a factor in the accelerated failure of these specimens.

CONCLUDING REMARKS

Isothermal oxidation kinetics of APS Ni-22Cr-10Al-1Y bond coatings were evaluated at 1150°C, as a function of YSZ presence and thickness. At up to 200 hours bare bond coatings continued to form an adherent scale, and the APS YSZ top coatings remained intact. Interfacial reaction products included Al_2O_3, $Ni(Cr,Al)_2O_4$ spinels, and slight amounts of Cr_2O_3. The bond coatings formed significant amounts of alumina and YAG as internal oxides. Thermal cycling resulted in differing failure modes as a function of YSZ thickness. Pre-oxidation significantly reduced cyclic lifetimes, indicating the influence of thermally activated processes on TBC degradation.

The next phase of the study will conduct similar experiments on specimens with single crystal superalloy substrates, LPPS NiCoCrAlY bond coatings and EB-PVD YSZ top coatings.

ACKNOWLEDGEMENTS

Research sponsored by the Assistant Secretary for Energy Efficiency and Renewable Energy, Office of Transportation Technologies, as part of the High Temperature Materials Laboratory Fellowship Program, Oak Ridge National Laboratory, managed by Lockheed Martin Energy Research Corp. for the U.S. Department of Energy under contract number DE-AC05-96OR22464.

REFERENCES

Alperine, S., and Lelait, L.,1994, "Microstructural Investigations of Plasma-Sprayed Yttria Partially Stabilized Zirconia TBC (In Relation to Thermomechanical Resistance and High-Temperature Oxidation Mechanisms)", *ASME Journal of Engineering for Gas Turbines and Power*, Vol. 116, pp. 258 - 265.

Bennett, A., 1986, "Properties of Thermal Barrier Coatings", 1986, *Materials Science and Technology*, Vol. 2, pp. 257 - 261.

Brindley, W. J., and Miller, R. A., 1990, "Thermal Barrier Coating Life and Isothermal Oxidation of Low-Pressure Plasma-Sprayed Bond Coat Alloys", *Surface and Coatings Technology*, 43/44, pp. 446-457.

De-Masi, J.T., Sheffler, K. D., Ortiz, M., 1989, "Thermal Barrier Coating Life Prediction Model Development', NASA CR182230.

Hillery, R. V., Pilsner, B. H., McKnight, R. L., Cook, T. S., and Hartle, M. S., 1988, "Thermal Barrier Coating Life Prediction Model Development", NASA CR180807.

Lelait, L., Alperine, S., and Mevrel, R., 1992, "Alumina Scale Growth at Zirconia-MCrAlY Interface: A Microstructural Study", *Journal of Materials Science*, Vol. 27, pp. 5 - 12.

Meier, S. M., Nissley, D. M., and Sheffler, K. D., 1991, "Thermal Barrier Coating Life Prediction Model Development", NASA Contractor Report 18911.

Mevrel, R., 1989, "State of the Art on High-Temperature Corrosion-Resistant Coatings", *Materials Science and Engineering*, A120, pp. 13-24.

Miller, R.A., 1984, "Oxidation-Based Model for Thermal Barrier Coating Life", *Journal of the American Ceramic Society*, Vol. 67, No. 8, pp. 517-521.

Miller, R.A., 1987, "Progress Toward Life Modeling of Thermal Barrier Coatings for Aircraft Gas Turbine Engines", *ASME Journal of Engineering for Gas Turbines and Power*, Vol. 109, pp. 448-451.

Miller, R.A., 1989, "Life Modeling of Thermal Barrier Coatings for Aircraft Gas Turbine Engines", *ASME Journal of Engineering for Gas Turbines and Power*, Vol. 111, p. 301-305.

Parks, W.F., Hoffman, E. E., Lee, W.Y., Wright, I.G., 1995, "Thermal Barrier Coatings Issues in Advanced Land-Based Gas Turbines", Proceedings of 1995 Thermal Barrier Coating Workshop, NASA Conference Publication 3312, pp. 35-47.

Prescott, R., and Graham, M. J., 1992, "The Formation of Aluminum Oxide Scales on High-Temperature Alloys", *Oxidation of Metals*, Vol. 38, Nos. 3/4, pp. 233-254.

Wortman, D. J., Nagaraj, B.A., and Duderstadt, E.C., 1989, "Thermal Barrier Coatings for Gas Turbine Use", *Materials Science and Engineering*, A121, pp. 433-440.

Wu, B.C., Chang, E., Chang, S.F., and Tu, D., 1989, "Degradation Mechanisms of ZrO_2-8wt% Y_2O_3/Ni-22Cr-10Al-1Y Thermal Barrier Coatings", *Journal of the American Ceramic Society*, Vol. 72, 2, p. 212-218.